

SOURCE
DATATRANSPARENT
PROCESSOPEN
ACCESS

RASSF1A is required for the maintenance of nuclear actin levels

Maria Chatzifrangkeskou¹ , Dafni-Eleftheria Pefani^{1,2,3} , Michael Eyres¹, Iolanda Vendrell^{1,4}, Roman Fischer⁴, Daniela Pankova¹ & Eric O'Neill^{1,*}

Abstract

Nuclear actin participates in many essential cellular processes including gene transcription, chromatin remodelling and mRNA processing. Actin shuttles into and out the nucleus through the action of dedicated transport receptors importin-9 and exportin-6, but how this transport is regulated remains unclear. Here, we show that RASSF1A is a novel regulator of actin nucleocytoplasmic trafficking and is required for the active maintenance of nuclear actin levels through supporting binding of exportin-6 (XPO6) to RAN GTPase. RASSF1A (Ras association domain family 1 isoform A) is a tumour suppressor gene frequently silenced by promoter hypermethylation in all major solid cancers. Specifically, we demonstrate that endogenous RASSF1A localises to the nuclear envelope (NE) and is required for nucleocytoplasmic actin transport and the concomitant regulation of myocardin-related transcription factor A (MRTF-A), a co-activator of the transcription factor serum response factor (SRF). The RASSF1A/RAN/XPO6/nuclear actin pathway is aberrant in cancer cells where RASSF1A expression is lost and correlates with reduced MRTF-A/SRF activity leading to cell adhesion defects. Taken together, we have identified a previously unknown mechanism by which the nuclear actin pool is regulated and uncovered a previously unknown link of RASSF1A and MRTF-A/SRF in tumour suppression.

Keywords exportin-6; MRTF-A; nuclear actin; nuclear envelope; RASSF1A

Subject Categories Cell Adhesion, Polarity & Cytoskeleton; Membrane & Intracellular Transport; Signal Transduction

DOI 10.15252/embj.2018101168 | Received 19 November 2018 | Revised 23 April 2019 | Accepted 14 May 2019

The EMBO Journal (2019) e101168

Introduction

Actin is one of the most highly conserved cytoskeletal proteins and found in all eukaryotic cells. The fundamental roles of actin are critical for biological processes such as determination of cell shape, vesicle trafficking and cell migration processes that are often

deregulated in transformed cells. Whilst the role of cytoplasmic actin is well established, the presence of nuclear actin is increasingly appreciated to play a crucial role in cellular responses to internal and external mechanical force (Guilluy *et al*, 2014). Nuclear actin is actively imported and exported through the activity of importin-9 (Dopie *et al*, 2012) and exportin-6 (Stuven *et al*, 2003) and has been implicated in transcription (Egly *et al*, 1984; Hofmann *et al*, 2004), cellular differentiation (Sen *et al*, 2015) and DNA repair (Belin *et al*, 2015). Nuclear actin monomers have been shown to directly regulate the myocardin-related transcription factor A (MRTF-A), a mechanosensitive co-factor of the serum response factor (SRF) transcription pathway (Vartiainen *et al*, 2007; Baarlink *et al*, 2013).

The Ras association domain family (RASSF) genes are upstream regulators of the Hippo tumour suppressor pathway. The family is composed of 10 members which are divided into two subgroups: (i) RASSF 1–6 possess a Ras association (RA) domain and a SARAH (Sav/Rassf/Hpo) protein–protein interaction domain in the C-terminus, and (ii) RASSF 7–10 also contain a RA domain at the N-terminus but lack a recognisable SARAH domain (Sherwood *et al*, 2010). The RA domains of the RASSF family bind K-RAS, H-RAS, RAP1/2 and RAN GTPases with varying affinity (Avruch *et al*, 2006; Dallol *et al*, 2009). The RASSF1A isoform is a *bona fide* tumour suppressor gene whose inactivation is implicated in the development of a wide range of human tumours including breast, lung and gastrointestinal cancer (Grawenda & O'Neill, 2015). Although gene deletion and germline mutations exist, the most widespread loss of RASSF1A function occurs through promoter hypermethylation-associated transcriptional silencing (Grawenda & O'Neill, 2015). RASSF1A directly binds Hippo kinases, mammalian sterile 20-like kinases 1 and 2 (MST1 and MST2) through the SARAH domain, promoting downstream Hippo pathway signalling to YAP1 (Guo *et al*, 2007; Matallanas *et al*, 2007). In response to DNA damage, nuclear RASSF1A is phosphorylated on Ser131 by ATM (ataxia-telangiectasia-mutated) or ATR (ATM- and Rad3-related) kinases, which promotes dimerisation and trans-autophosphorylation of MST2 required for its activation (Hamilton *et al*, 2009; Pefani *et al*, 2014). Plasma membrane localisation of cytoplasmic RASSF1A occurs in response to growth factor signalling or direct RAS

¹ Department of Oncology, University of Oxford, Oxford, UK

² Laboratory of Biology, Medical School, National and Kapodistrian University of Athens, Athens, Greece

³ Biomedical Research Foundation of the Academy of Athens, Athens, Greece

⁴ Nuffield Department of Medicine, Target Discovery Institute, University of Oxford, Oxford, UK

*Corresponding author. Tel: +44 1865617321; E-mail: eric.oneill@oncology.ox.ac.uk

association with the RA domain (Pefani *et al*, 2016). However, the localisation of RASSF1A to mitotic structures has been attributed to RA domain binding to tubulin (also a GTP-binding protein) and is a

likely cause of hyperstabilisation of tubulin commonly observed in interphase cells overexpressing exogenous levels (Liu *et al*, 2003; Dallol *et al*, 2004; Vos *et al*, 2004; El-Kalla *et al*, 2010).

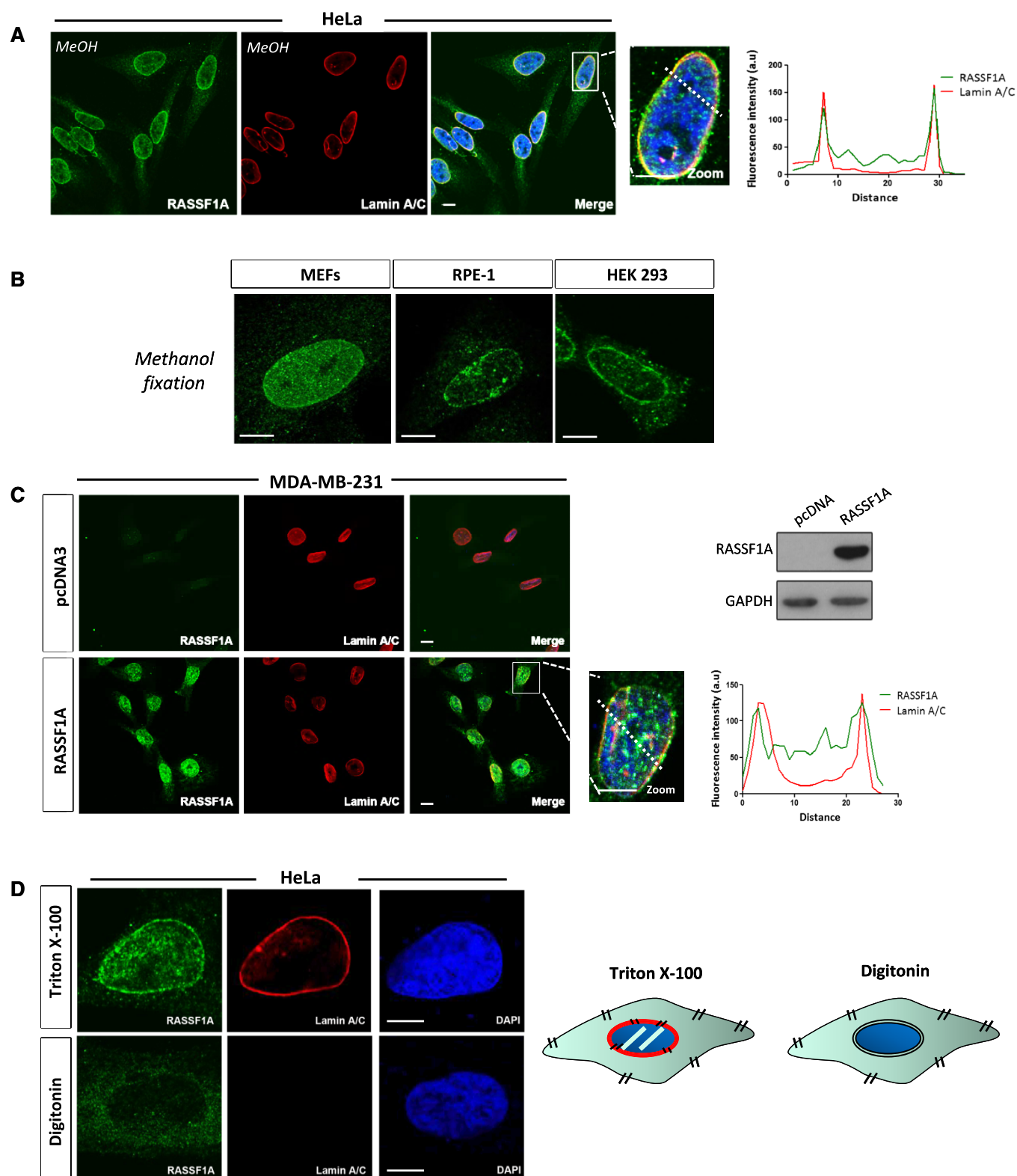


Figure 1.

Figure 1. RASSF1A localises at the inner nuclear membrane.

- A Representative confocal images of RASSF1A localisation in HeLa cells. Nuclear DNA was stained with DAPI. Fluorescence intensity profile of Lamin A/C (red) and RASSF1A (green) signals across the HeLa nuclei. Position of line scan indicated by the dashed white line. Scale bars = 10 μ m.
- B Immunofluorescence images of endogenous RASSF1A expression in mouse embryonic fibroblasts (MEFs) (left), human retinal pigmented epithelial RPE-1 cells (middle) and human embryonic kidney HEK293 cells (right). Scale bars = 10 μ m.
- C Co-staining of endogenous RASSF1A expression in MDA-MB-231 cells transfected with the pcDNA3 expressing RASSF1A. Western blot analysis shows the protein levels of RASSF1A following plasmid transfection. Fluorescence intensity profile of Lamin A/C (red) and RASSF1A (green) signals across the HeLa nuclei. Position of line scan indicated by the dashed white line. Scale bars = 10 μ m.
- D *Left*: representative confocal images of HeLa cells permeabilised either with Triton X-100 (top panels) or with digitonin (bottom panels) and stained for RASSF1A, Lamin A/C and DNA (DAPI). Scale bars = 10 μ m. *Right*: schematic representation of the cellular membranes permeabilised with Triton X-100 and digitonin.

Source data are available online for this figure.

Here, we show that nuclear RASSF1A is recruited to the NE by a lamina-associated pool of the Hippo kinase, MST2. Furthermore, we find that RASSF1A is required for the association of exportin-6 (XPO6) with RAN GTPase, the nuclear export of the XPO6 cargoes, actin and profilin, an actin-binding protein involved in the dynamic sensing of the actin cytoskeleton and the regulation of the MRTF-A/SRF axis. Tumour cells lacking RASSF1A expression display high levels of nuclear actin/profilin, reduced MRTF-A levels and low transcription of SRF target genes, including SRF itself. In line with these findings, we find that human tumours display a high level of correlation between RASSF1A and SRF expression, with evidence for low SRF mRNA as a poor prognostic factor in breast and liver cancers. These events reveal the potential primary mechanism for the tumour suppressor RASSF1A in cancer being mediated through deregulation of nuclear actin transport.

Results

RASSF1A localises at the inner nuclear membrane

RASSF1A acts as a microtubule-associated protein that stabilises microtubules (Liu *et al*, 2003; Dallol *et al*, 2004; Vos *et al*, 2004; El-Kalla *et al*, 2010). However, these phenotypes were determined after the accumulation of overexpressed protein over a 24- to 48-h period. To identify the localisation of endogenous nuclear RASSF1A by indirect immunofluorescence (IF) and methanol fixation, we used an anti-RASSF1A antibody (ATLAS), the specificity of which was validated in cells depleted for RASSF1A (Figs EV1A and B). Interestingly, in HeLa cells endogenous RASSF1A is distributed predominantly throughout the nuclear interior and at the perinuclear regions. Co-staining of RASSF1A and the inner nuclear membrane (INM) protein Lamin A/C showed a high degree of co-localisation and similar fluorescence intensity profiles (Fig 1A). Silencing of RASSF1A resulted in loss of the nuclear ring staining, indicating that the fluorescence signal is specific for RASSF1A (Fig EV1B). Localisation was conserved across multiple cell types including mouse embryonic fibroblasts (MEFs), human retinal pigmented epithelial RPE-1 cells and human embryonic kidney HEK 293 cells (Fig 1B). The RASSF1A gene promoter is highly methylated in the breast carcinoma cell line MDA-MB-231 and therefore significantly downregulated (Montenegro *et al*, 2012). Concomitantly, no immunofluorescence was observed in MDA-MB-231 cells, but upon transient transfection with a plasmid expressing RASSF1A, NE localisation of the exogenous protein was evident (Fig 1C). Alternatively,

treatment of MDA-MB-231 with the demethylating agent 5'-aza-dC led to the re-expression of endogenous RASSF1A and yielded similar staining (Fig EV1C).

To further assess the localisation of RASSF1A in relation to the structure of the NE, HeLa cells were treated with either Triton X-100 or digitonin. Whereas Triton X-100 is used to permeabilise all cellular membranes, digitonin can permeabilise preferentially the plasma membrane of cultured cells and leave the NE intact. Therefore, only proteins of the outer nuclear membrane (ONM) that face the cytoplasm are detectable in digitonin-permeabilised cells. In Triton X-100-permeabilised HeLa cells, RASSF1A co-localises with Lamin A/C (Fig 1D). In contrast, neither Lamin A/C nor RASSF1A was detected at the nuclear envelope in digitonin-permeabilised cells. Permeabilisation of the plasma membrane of the digitonin-treated cells was validated using co-staining of RASSF1A with α -tubulin, a marker of cytoplasm (Fig EV1D). These results support the hypothesis that RASSF1A localises at the inner nuclear membrane (INM) of the NE.

The ATM and ATR kinases catalyse phosphorylation of RASSF1A at Ser131 to regulate its activity (Hamilton *et al*, 2009). Phosphorylated (Ser131) RASSF1A was present within the nucleus and at the INM of HeLa cells (Fig EV1E). To determine whether phosphorylation of RASSF1A on Ser131 by ATM and ATR kinases is required for its localisation at the inner nuclear membrane, HeLa cells were treated with the ATR inhibitor (VE-821) or ATM inhibitor (KU55933). Inhibition of ATR, ATM or combined ATR/ATM activity did not abolish RASSF1A perinuclear localisation (Fig EV1F). Collectively, the above observations show that the RASSF1A association with the NE is specific and not dependent on the kinase activity of ATR and ATM kinases.

RASSF1A localisation at the NE is mediated by MST2

RASSF1A directly binds mammalian STE20-like protein kinases 1 and 2 (MST1 and MST2) to support maintenance of MST1/2 phosphorylation and activation (Sánchez-Sanz *et al*, 2016). Interestingly, mass spectrometry analysis of MST2 eluted fractions from HeLa lysates identified confidently the interaction between MST2 and Lamin A/C (Figs 2A and EV2A) and suggested a potential interaction with Lamin B1. We further examined the cellular localisation of nuclear MST1/2 kinases by IF in HeLa cells (with methanol fixation) and we observed that only MST2 (ab71960), and not MST1, exhibited perinuclear distribution similar to RASSF1A, as shown with co-staining with Lamin B1 (Fig 2B). The perinuclear staining of MST2 was confirmed using another antibody (ab52641) recognising the

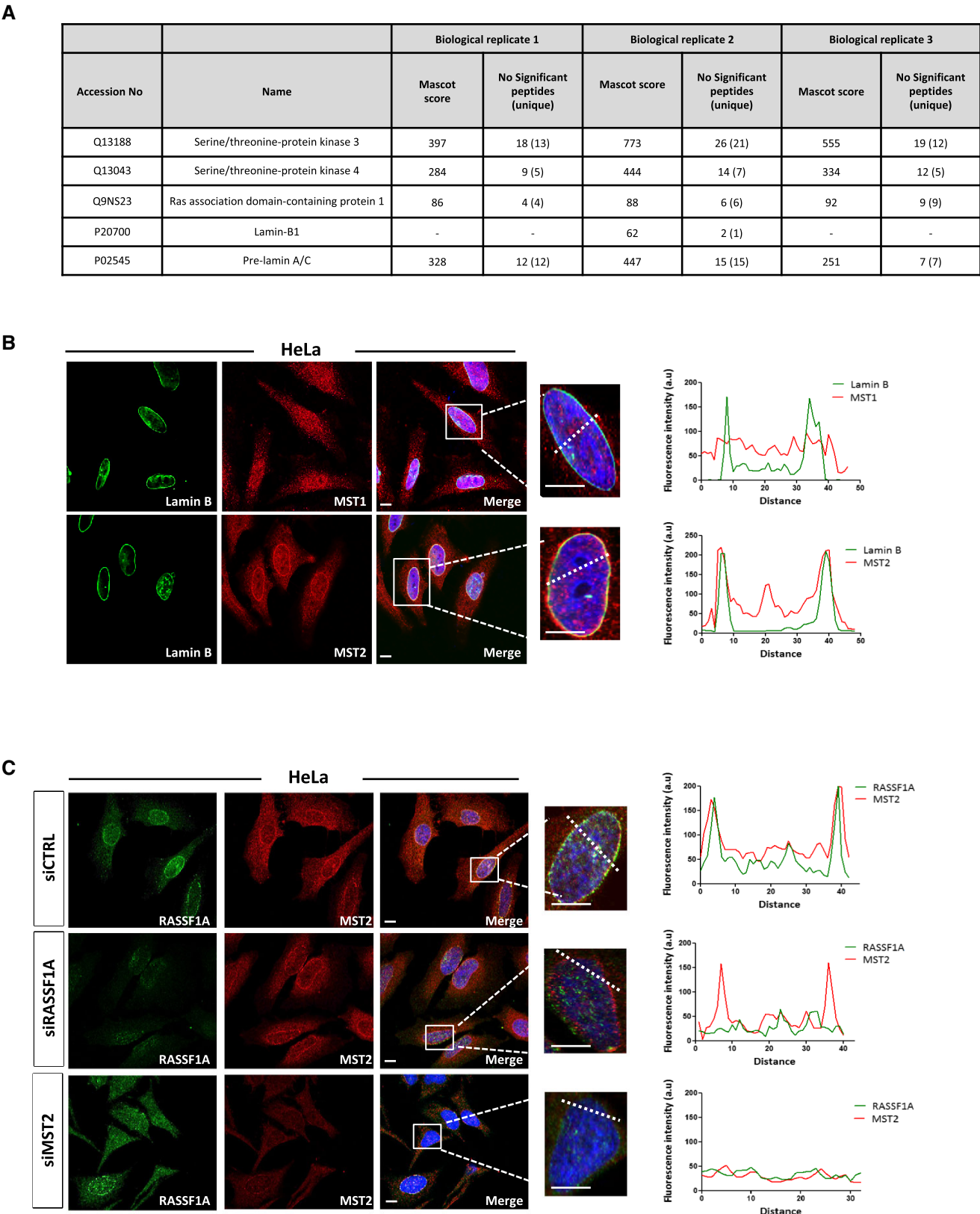


Figure 2.

Figure 2. RASSF1A localisation at the NE is mediated by MST2.

- A List of proteins identified by LC-MS/MS in MST2 IP. The table includes the MASCOT score and number of significant peptides and unique peptides (in brackets) identified in each biological replicates after applying a 20 ion cut-off and 1% FDR rate. Lamin B1 was identified only in 1 out of the 3 biological replicates with 1 unique peptide. However, interactions were verified by WB (Fig EV2A).
- B Representative confocal images of MST1 (top) and MST2 (bottom) co-stained with the nuclear envelope marker Lamin B. DNA was stained with DAPI. Fluorescence intensity profile of Lamin B (green) and MST1 or MST2 (red) signals across the HeLa nuclei. Position of line scan indicated by the dashed white line. Scale bars = 10 μ m.
- C Immunofluorescence images of RASSF1A and MST2 in siCTRL-, siRASSF1A- and siMST2-treated cells. DNA was stained with DAPI. The graphs illustrate the fluorescence intensity profile of Lamin B (green) and MST2 (red) signals along the white lines shown in the merged panels. Scale bars = 10 μ m.

N-terminus (Fig EV2B). To explore the role of MST2 localisation at the NE in relation to RASSF1A, we next reduced MST2 expression using siRNA-mediated knockdown and observed substantial reduction in RASSF1A staining at the INM in the absence of MST2 without affecting the overall nuclear RASSF1A protein levels (Fig EV2C and D). Conversely, RASSF1A knockdown did not affect MST2 NE distribution (Fig 2C). Overall, these results suggest that MST2 mediates RASSF1A localisation at the INM via lamina association.

RASSF1A binds to XPO6 through its SARAH domain

We previously showed that RASSF1A interacts with RAN GTPase (Dallol *et al*, 2009), a key component in the regulation of nucleocytoplasmic transport. Given our data above showing the localisation of RASSF1A in the INM, we now sought to identify whether RASSF1A plays an active role in the process of RAN-dependent nuclear export. To test our hypothesis, we performed immunoprecipitation using extracts of HeLa cells and antibodies against exportin-1 (CRM1/XPO1), exportin-4 (XPO4), exportin-5 (XPO5), exportin-6 (XPO6) and exportin-7 (XPO7; Fig 3A). Interestingly, we found that RASSF1A specifically interacts with XPO6, but not with CRM1/XPO1 which is the most conserved and responsible for export of a wide variety of cargoes (Fornerod *et al*, 1997).

In order to determine the domain responsible for its interaction with XPO6, we exogenously expressed full-length MYC-RASSF1A and different RASSF1A-truncated mutants in HeLa cells. Whereas full-length MYC-RASSF1A (aa 1–340) and MYC-RASSF1A (aa 120–340) could specifically precipitate XPO6, no signal was detected with mutants lacking the SARAH domain, MYC-RASSF1A (aa 1–288) and MYC-RASSF1A (aa 120–288; Fig 3B). Overall, these data demonstrate that the SARAH domain of RASSF1A is required for the interaction with XPO6.

We further investigated the role of RASSF1A on the association of RAN with XPO6. Most strikingly, RASSF1A appeared to be required to support the XPO6/RAN complex, as siRNA-mediated knockdown of RASSF1A decreased association between XPO6 and RAN (Fig 3C). Expression of RASSF1A in MDA-MB-231 cells significantly enhances the association of XPO6 with RAN (Fig EV3A). We validated this requirement for RASSF1A with a GST pull-down assay using recombinant GST-RAN and lysates from siCTRL or siRASSF1A-transfected HeLa cells (Fig EV3B). Notably, XPO6 co-immunoprecipitation (IP) indicated that the XPO6/RAN complex with RASSF1A also includes MST2, suggesting potential recruitment to the NE via the RASSF1A-MST2 interaction (Fig 3C). Depletion of MST2 expression using siRNA did not affect XPO6/RAN as dramatically as siRASSF1A, but did reduce XPO6/RASSF1A, which we believe implies that

RASSF1A may be required for stabilising XPO6/RAN at the NE, i.e. in an MST2-dependent manner, but the nucleoplasmic XPO6/RAN pool may be less dependent on RASSF1A (Fig 3C). This is supported by the fact that the RASSF1A interaction with XPO6/RAN is also dependent on MST2 and therefore NE localisation (Fig 3D). To verify this mechanism, we explored MST2 associated proteins by IP and found that XPO6/RAN interaction with MST2 was RASSF1A-dependent whereas the RASSF1A/RAN interaction with MST2 did not require XPO6 (Fig EV3C), confirming our hypothesis that XPO6/RAN complex is stabilised by MST2/RASSF1A interaction. Taken together, our results show interaction of XPO6 with RAN can occur independently of RASSF1A, but a pool of XPO6/RAN is stabilised by RASSF1A in a MST2-dependent manner at the NE.

RASSF1A is involved in actin and profilin nuclear export process

XPO6 mediates specifically the export of actin and profilin complexes out of the nucleus (Stuven *et al*, 2003). We next determined whether RASSF1A plays a role in the XPO6-dependent nuclear export. Interestingly, subcellular nuclear/cytoplasmic fractionation of HeLa cell lysates clearly demonstrated elevated levels of profilin and actin in the nucleus upon siRNA-mediated silencing of RASSF1A, compared to cells treated with control siRNA, suggesting an impaired nuclear export (Fig 4A). To further validate these results, increase in nuclear actin and profilin in RASSF1A silenced cells was only rescued upon co-transfection of RASSF1A derivatives containing a SARAH domain or overexpression of XPO6 (Fig EV4A and B). Furthermore, to ensure these effects were specific to RASSF1A, we restored nuclear actin and profilin export with siRNA-resistant FLAG-RASSF1A (Fig EV4C). Nuclear retention of profilin in HeLa cells treated with siRNA against RASSF1A was further demonstrated by immunofluorescence (Fig 4B). Remarkably, silencing of MST2 led to altered nuclear levels of actin and profilin similar to RASSF1A depletion, indicating that the NE localisation of RASSF1A is important for regulation of XPO6 (Fig EV4D). Importantly, RASSF1A gene silencing does not affect the expression levels of XPO6 (Fig EV4E). To rule out the possibility that nuclear actin accumulation resulted from impaired nuclear import receptor levels, we next examined protein expression of importin-9 (IPO9), which is required for actin translocation to the nucleus (Dopie *et al*, 2012), in the absence of RASSF1A. Western blotting showed no change in the expression of IPO9 upon depletion of RASSF1A, compared with the siCTRL-transfected cells (Fig EV4E). We next wondered whether the increased nuclear actin exists in monomeric (G-actin) or filamentous state (F-actin). We visualised nuclear F-actin using 568-conjugated phalloidin and G-actin using 488-conjugated DNase I. Although we did not detect any difference in the

F-actin between siCTRL- and si-RASSF1A-treated cells, we observed that significant increase in G-actin in RASSF1A-depleted cells (Figs 4C and EV4F). The significance of RASSF1A for XPO6-

mediated export process is also evident in MDA-MB-231 cells that lack RASSF1A expression. Strikingly, forcing the expression of RASSF1A either by transiently transfecting MDA-MB-231 cells with

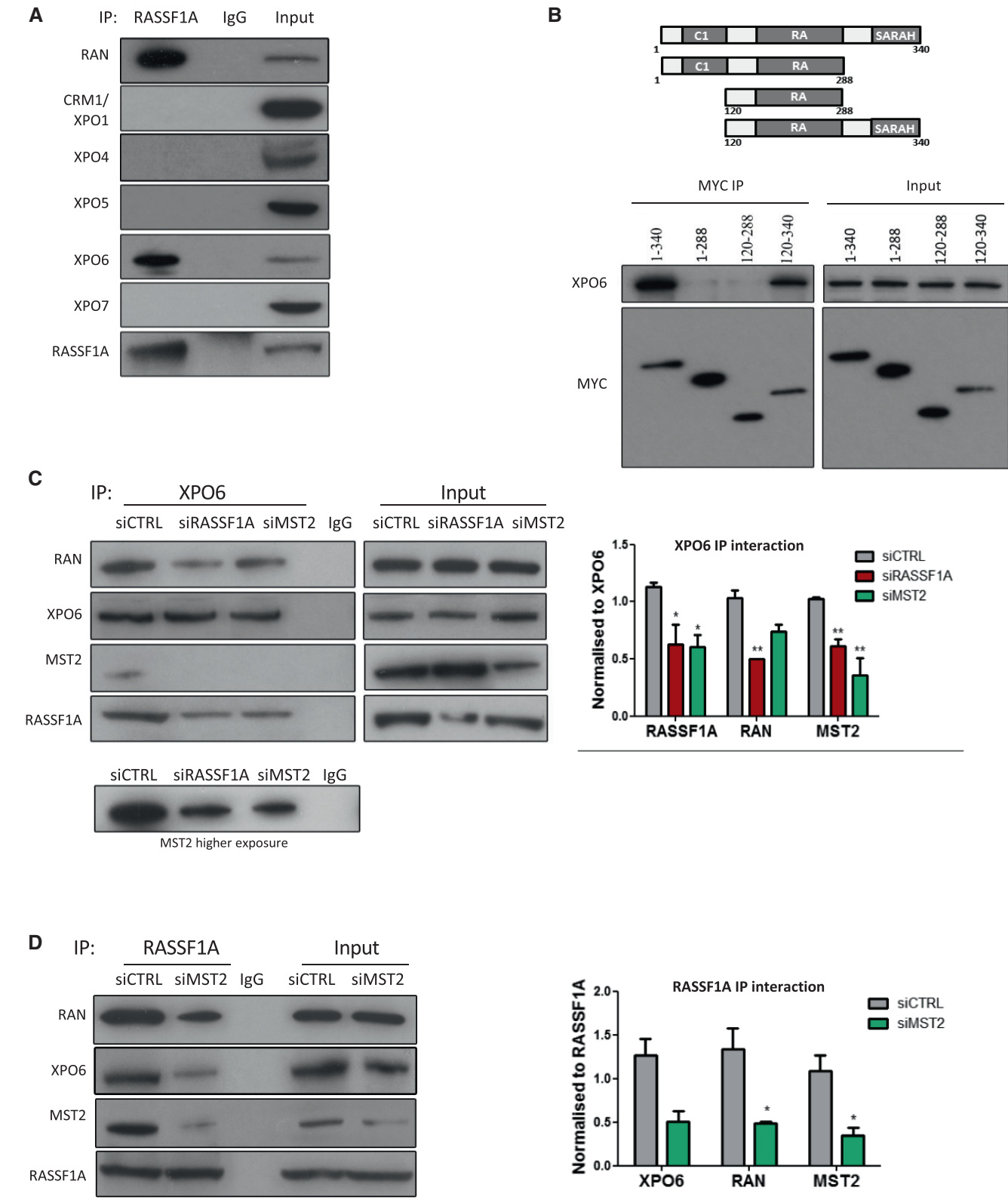


Figure 3.

Figure 3. RASSF1A binds to XPO6 through its SARAH domain.

- A Co-immunoprecipitation of endogenous RASSF1A with endogenous RAN, CRM1/XPO1, XPO4, XPO5, XPO6 and XPO7 from HeLa cell lysates, compared with the IgG control.
- B *Upper*: graphical representation of the domain structure of full-length RASSF1A and mutant constructs used for mapping RASSF1A/XPO6 interaction. Different domains are abbreviated as follows: SARAH, Salvador-RASSF-Hippo domain; C1, N-terminal C1 type zinc fingers; and RA, Ras-binding domain. *Lower*: Western blot analysis of MYC immunoprecipitation from the indicated inputs from HeLa cells. Co-immunoprecipitation of endogenous XPO6 with RAN in siRASSF1A from HeLa cell lysates.
- C Co-immunoprecipitation of endogenous XPO6 with endogenous RAN, RASSF1A and MST2 in siRASSF1A and siMST2 HeLa cells. Quantification of the interaction of XPO6 with RASSF1A, RAN and MST2 relative to XPO6 is shown. Error bars derive from three independent experiments and represent the SEM.
- D Co-immunoprecipitation of endogenous RASSF1A with endogenous XPO6 and RAN in siRNA-mediated knockdown of MST2 HeLa cells. Quantification of the interaction of RASSF1A with XPO6, RAN and MST2 relative to RASSF1A is shown. Error bars derive from three independent experiments and represent the SEM.
- Data information: Two-tailed Student's t-test was used for statistical analysis. * $P < 0.05$, ** $P < 0.01$.
 Source data are available online for this figure.

a plasmid encoding *RASSF1A* or by treating cells with the demethylating agent 5'-aza-dC led to a decrease in actin and profilin nuclear retention (Figs 4D and EV4G). Taken together, these data strongly indicate that *RASSF1A* governs the export of actin and profilin out of the nucleus.

Loss of RASSF1A expression alters MRTF-A/SRF axis

Previous studies showed that nuclear actin has been linked to gene transcription (Visa & Percipalle, 2010; Grosse & Vartiainen, 2013; Kapoor & Shen, 2014), downregulating the expression of *MYL9*, *ITGB1* and *PAK1* (Sharili et al, 2016). Therefore, we measured mRNA levels of these nuclear actin-regulated genes and show that these genes were significantly reduced following siRNA-mediated knockdown of *RASSF1A* in comparison with control (siCTRL) HeLa cells (Fig 5A). Furthermore, mRNA encoding the transcription factor *OCT4*, which is known to be activated by nuclear actin (Yamazaki et al, 2015), was elevated in HeLa cells depleted of *RASSF1A* (Fig 5A). It is well established that depletion of IPO9 inhibits nuclear import of actin (Dopie et al, 2012). As expected, the levels of actin in nuclear extracts from HeLa cells treated with siRNA against IPO9 were decreased and prevented accumulation even in the absence of export via *RASSF1A* silencing (Fig EV5B). Moreover, the levels of *MYL9*, *ITGB1*, *PAK1* and *OCT4* mRNA upon *RASSF1A* silencing were rescued in HeLa cells co-depleted of IPO9 (Fig 5A).

We next tested whether increased nuclear actin levels arising from *RASSF1A* depletion have functional consequences for the cells. Since multiple nuclear actin-regulated genes encode for known regulators of cell adhesion (Sharili et al, 2016), we then assessed whether these cellular functions are affected in *RASSF1A*-depleted cells. In accordance with our qRT-PCR data, we showed that HeLa cells lacking *RASSF1A* exhibited a significantly decreased number of adhesive cells (Fig 5B). Accordingly, restoring actin levels in the nucleus by silencing IPO9 in the absence of *RASSF1A* was sufficient to rescue this effect (Fig 5B). Collectively, our data show that *RASSF1A* has an indirect effect on the expression of genes involved in cell adhesion processes, via regulation of actin levels within the nucleus.

Nuclear actin plays a key role in the regulation of the localisation and activity of myocardin-related transcription factor A (MRTF-A), a co-activator of the transcription factor serum response factor (SRF), which regulates the expression of many cytoskeletal genes (Sotiropoulos et al, 1999; Miralles et al, 2003;

Vartiainen et al, 2007; Ho et al, 2013). We next hypothesised that both MRTF-A localisation and transcriptional activity of SRF could be affected by *RASSF1A* protein levels. Notably, we observed that MRTF-A resides mostly in the cytoplasm in the absence of *RASSF1A*, whereas it is located in both nucleus and cytoplasm in control cells (Fig 5C). These observations are in line with our findings showing increased monomeric G-actin levels in *RASSF1A*-depleted cells as G-actin binds to MRTF-A and promotes its nuclear export (Miralles et al, 2003; Vartiainen et al, 2007). In agreement with these studies, we also showed an increased interaction between actin and MRTF-A in siRASSF1A-treated cells (Fig EV5C). Furthermore, increased nuclear G-actin levels exclude MRTF-A from the nucleus and block SRF-dependent gene transcription (Posern et al, 2002; Vartiainen et al, 2007). Accordingly, we showed decreased mRNA levels of the *SRF* gene together with decreased FBS-stimulated SRF reporter activity in cells transfected with siRNA against *RASSF1A* (Figs 5D and EV5D). Silencing IPO9 restored MRTF-A nuclear localisation and SRF expression in *RASSF1A*-depleted cells (Fig 5C and D). These results demonstrate a correlation between *RASSF1A* expression and SRF axis regulation, via actin localisation.

Correlation of RASSF1 and SRF expression in human tumours

We next analysed *SRF* gene expression from clinical data available from The Cancer Genome Atlas (TCGA) database with the cBioPortal tool (<http://www.cbioportal.org>). *RASSF1A* promoter methylation is widely appreciated to correlate with adverse prognosis, and we find a significant correlation between this epigenetic event and *SRF* mRNA levels indicating that loss of nuclear actin regulation and MRTF-A/SRF is likely to contribute to clinical parameters (Fig 6A, top). In line with a role in tumour suppression, *SRF* levels are significantly reduced in invasive breast cancer compared with control normal tissues (Wilcoxon $P = 1.164 \times 10^{-20}$; Fig 6B, bottom). Additionally, breast invasive carcinomas (TCGA) display higher *SRF* mRNA expression in tumours with high levels of *RASSF1A* transcript ($P < 0.0001$), which also shows significant linear correlation across the dataset ($R = 0.28$; Fig 6B). We find a matching association of *RASSF1A* and *SRF* in hepatocellular carcinoma (TCGA; $P < 0.0001$), again with significant linear correlation of *RASSF1A*/*SRF* transcripts ($R = 0.29$; Fig 6C) and further correlations with bladder and colorectal cancer (Fig EV6). Notably, *SRF* mRNA levels were enriched in the *RASSF1A*^{high} individuals in four distinct cancer types (Figs 6 and EV6). Finally, we examined the breast and liver cancer

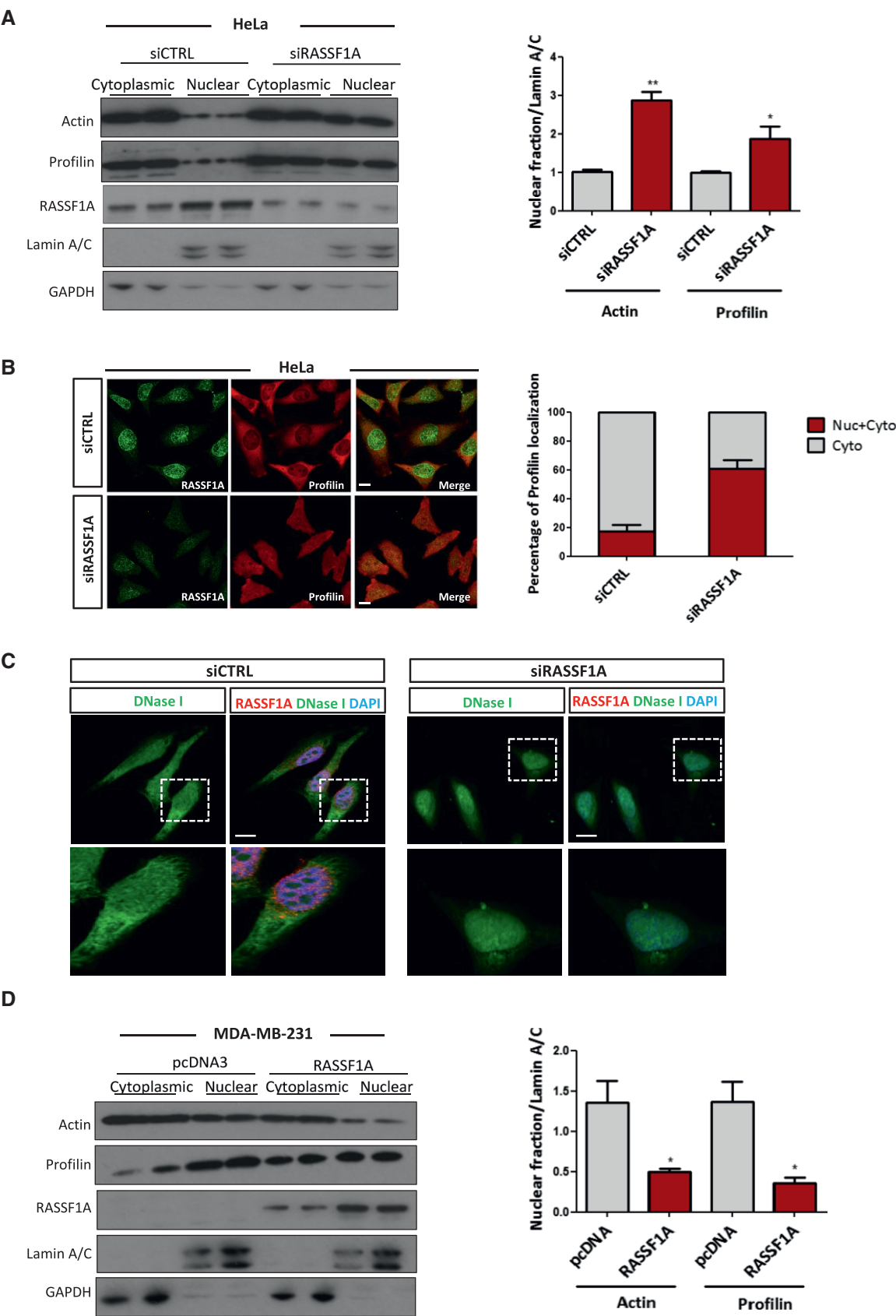


Figure 4.

Figure 4. RASSF1A is involved in actin and profilin nuclear export process.

- A HeLa cells treated with control or RASSF1A siRNA were fractionated into cytoplasmic and nuclear extracts. Lysates from each fraction were probed for actin and profilin alongside GAPDH (as a marker of the cytoplasmic fraction) and Lamin A/C (as a marker of the nuclear fraction). *Right*: quantification of nuclear actin and profilin relative to Lamin A/C is shown. Error bars derive from two independent experiments and represent the SEM.
- B Immunofluorescence images of profilin in control and RASSF1A siRNA-transfected HeLa cells. *Right*: the profilin localisation was scored as nuclear/cytoplasmic or predominantly cytoplasmic in approximately 100 cells. Error bars derive from three independent experiments and represent the SEM.
- C Confocal images of endogenous monomeric globular actin (G-actin) in siCTRL and siRASSF1A cells using DNase I staining (Alexa Fluor 488-conjugated, green). Scale bars = 10 μ m.
- D Western blot analysis of actin, profilin, GAPDH and Lamin A/C levels in nuclear and cytoplasmic fractions of MDA-MB-231 cells treated with control pcDNA3 or RASSF1A vector. The graph shows the nuclear levels of actin and profilin relative to Lamin A/C in MDA-MB-231 cells expressing RASSF1A. Error bars derive from two independent experiments and represent the SEM.

Data information: Two-tailed Student's t-test was used for statistical analysis. * $P < 0.05$, ** $P < 0.01$.
 Source data are available online for this figure.

survival statistics in the TCGA and we found that patients with low SRF expression have a poor prognosis for overall survival (Breast HR = 0.8 (0.72–0.89) Logrank $P = 5e^{-5}$; HCC HR = 0.67 (0.47–0.96) Logrank $P = 0.027$; Fig 6D). Overall, our data show a correlation of RASSF1 and SRF mRNA expression and SRF levels associate with poor survival.

Discussion

Actin constantly shuttles between the cytoplasm and the nucleus using an active transport mechanism, and proper balance of nuclear and cytoplasmic actin pools is tightly regulated. Nuclear actin is exported from the nucleus by XPO6, independently of the general export receptor CRM1, and it is imported by IPO9 (Stuven *et al*, 2003; Dopie *et al*, 2012). As for most export processes, XPO6 also requires RAN GTPase to export actin monomers in complex with profilin from the nucleus (Stuven *et al*, 2003). We found that lack of RASSF1A, a phenomenon commonly observed in human tumours, leads to accumulation of actin within the nucleus due to defective nuclear export. The direct interaction of RASSF1A with XPO6, a member of the importin- β superfamily of transport receptors, is required for the association with RAN. Intriguingly, the RASSF1A/RAN/XPO6 complex includes MST2, suggesting that the recruitment of RASSF1A to MST2 at the NE potentially supports XPO6 binding via the SARA domain (Dittfeld *et al*, 2012) and this is important for the active participation in actin-profilin nucleocytoplasmic shuttling. However, the reduced involvement of RASSF1A in the XPO6/RAN complex in the absence of MST2 suggests that RAN/XPO6 exists independently of RASSF1A in the nucleoplasm. This means that XPO6/RAN complexes may be contextually distinct from RASSF1A/RAN/XPO6 and could involve differences in substrate loading, RAN GDP/GTP loading or post-translational modifications of RAN (Dallol *et al*, 2009; Bompard *et al*, 2010; Güttler & Görlich, 2011; de Boer *et al*, 2015).

Reduction in cytoplasmic actin was not evident as a consequence of the defective export, most likely because of the higher actin concentration in the cytoplasm (Fig 4A). Nuclear actin is a key regulator of transcription, and it is required for all three RNA polymerases (Pol I, II and III; Philimonenko *et al*, 2004; Qi *et al*, 2011). Previous reports showed that expression of nuclear actin negatively regulates multiple genes and results in altered expression of approximately 2,000 genes (Yamazaki *et al*, 2015; Sharili *et al*, 2016). Loss of RASSF1A expression alters gene expression

and impacts cellular processes, such as cell adhesion. Thus, RASSF1A appears to contribute to the transcriptional activity of the cell and further to its phenotypic changes through its ability to modulate nuclear actin levels. Although nuclear actin levels have not been extensively studied in cancer cells, abnormal subcellular localisation of certain ABPs (actin-binding proteins) is associated with the development carcinogenesis processes (Loy *et al*, 2003; Velkova *et al*, 2010; Khurana *et al*, 2011; Savoy & Ghosh, 2013; Honda, 2015; Patnaik *et al*, 2016). A recent study showed that the nuclear actin levels regulated by XPO6 are pivotal for cell proliferation and quiescence and that preventing actin export from the nucleus contributes to malignant progression (Fiore *et al*, 2017). Of note, low XPO6 expression and therefore nuclear actin accumulation correlate with poor survival of breast cancer patients (Fiore *et al*, 2017).

Mechanotransduction signalling is essential for a broad range of biological functions such as embryogenesis, cell migration, metastasis and epithelial–mesenchymal transition. MRTF-A is a mechanosensitive transcription co-factor which, together with SRF, controls a variety of genes involved in actin cytoskeletal remodelling and growth factor response. MRTF-A/SRF activation is responsible for immediate transcriptional response to mechanical stimuli (Cui *et al*, 2015) and perturbed MRTF-A/SRF signalling axis might partially explain the pathogenesis of certain human diseases (Ho *et al*, 2013). We found that the SRF-driven gene transcription activity in response to serum stimulation was severely abrogated in RASSF1A-depleted cells (Fig 5D). In addition, we also found that RASSF1 expression correlates with SRF expression in a variety of cancers (Fig 6). Although there is currently lack of evidence, altered MRTF-A/SRF signalling may explain the aberrant mechanosensitivity observed often in cancer cells (Ghosh *et al*, 2008; Tang *et al*, 2012; Ciasca *et al*, 2016).

Epigenetic silencing of the RASSF1A gene has been frequently associated with poor patient outcome across all solid malignancies (Grawenda & O'Neill, 2015). Several studies have identified functional roles for RASSF1A-mediated tumour suppression that can explain these clinical associations, e.g. Hippo pathway regulation (Matallanas *et al*, 2007; Hamilton *et al*, 2009), apoptosis (Vos *et al*, 2000; Baksh *et al*, 2005), differentiation (Papaspypopoulos *et al*, 2018), the cytoskeleton (Liu *et al*, 2003; Dallol *et al*, 2004; Vlahov *et al*, 2015) and DNA damage/repair (Pefani *et al*, 2014, 2018; Donninger *et al*, 2015). However, the widespread prognostic associations imply a perturbation of a biological process that simultaneously contributes to these diverse

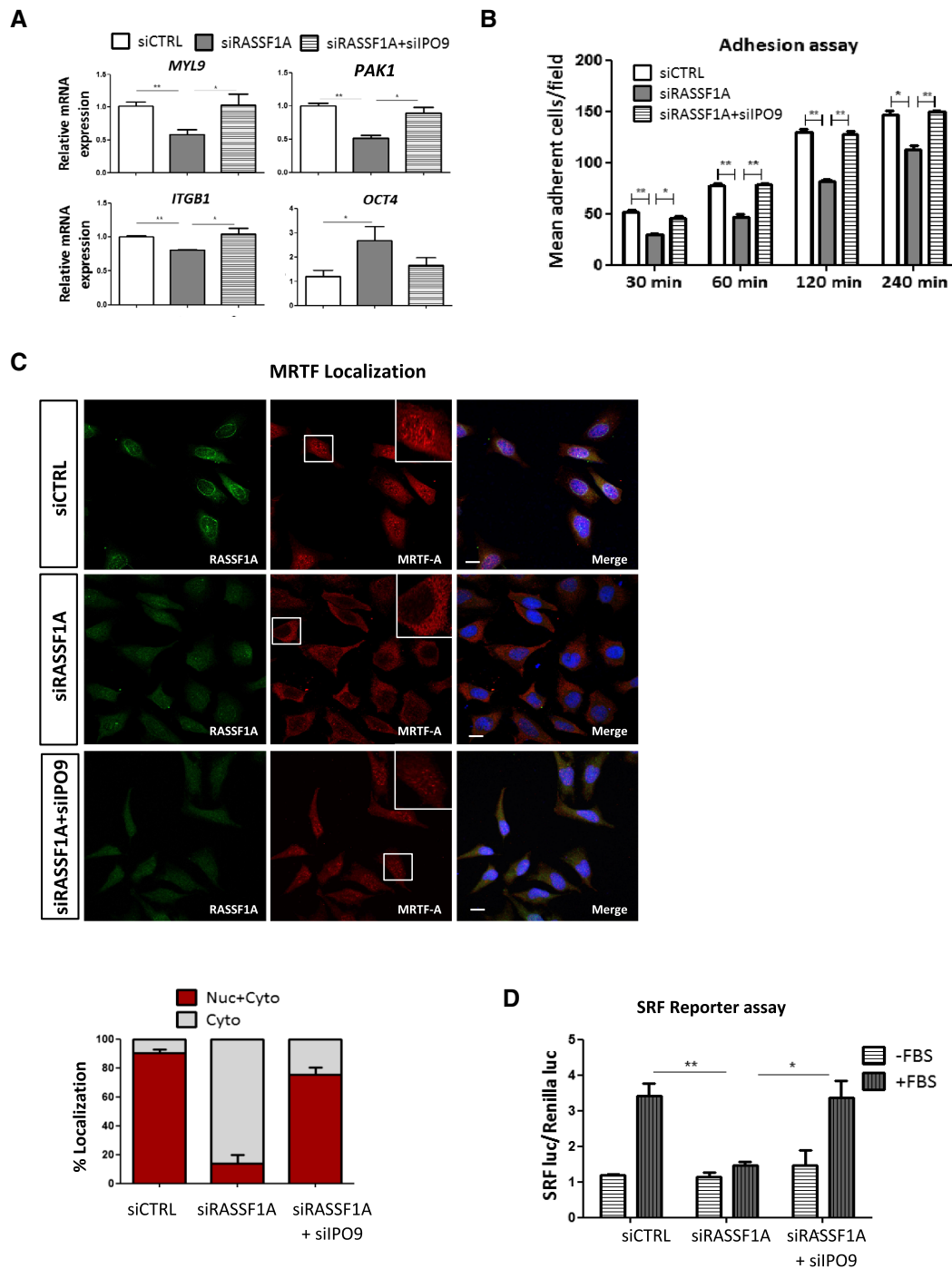


Figure 5. Loss of RASSF1A expression alters MRTF-A/SRF axis.

A qRT-PCR validation of selected genes known to be affected by the levels of nuclear actin. Transcript levels of *MYL9*, *ITGB1*, *PAK1* and *OCT4* from HeLa cells treated either with siRASSF1A or with siRASSF1A + siIPO9 are relative to *GAPDH* and normalised to siCTRL cells. Data represent SEM of three independent experiments.

B Adhesion assay. siRNA against *RASSF1A* significantly decreased HeLa cells' adhesive rate at all the determined time points compared with control. The cells were cultured for 48 h before harvesting and reseeding for 1 h on 96-well plates coated with FN. Data represent the SEM of three independent experiments.

C Representative immunofluorescence images of MRTF-A localisation in siRASSF1A and siRASSF1A + siIPO9. Lower: the MRTF-A localisation was scored as nuclear/cytoplasmic or predominantly cytoplasmic in 100–200 cells. DNA was stained with DAPI. Error bars derive from two independent experiments and represent the SEM. Scale bars = 10 μ m.

D Luciferase assay of SRF-dependent promoter in cells transfected with siCTRL, siRASSF1A or siRASSF1A + siIPO9 following stimulation with 10% FBS for 5 h. Data are expressed as SRF luciferase activity relative to Renilla control and represent the SEM of two independent experiments.

Data information: Two-tailed Student's t-test was used for statistical analysis. * $P < 0.05$, ** $P < 0.01$.

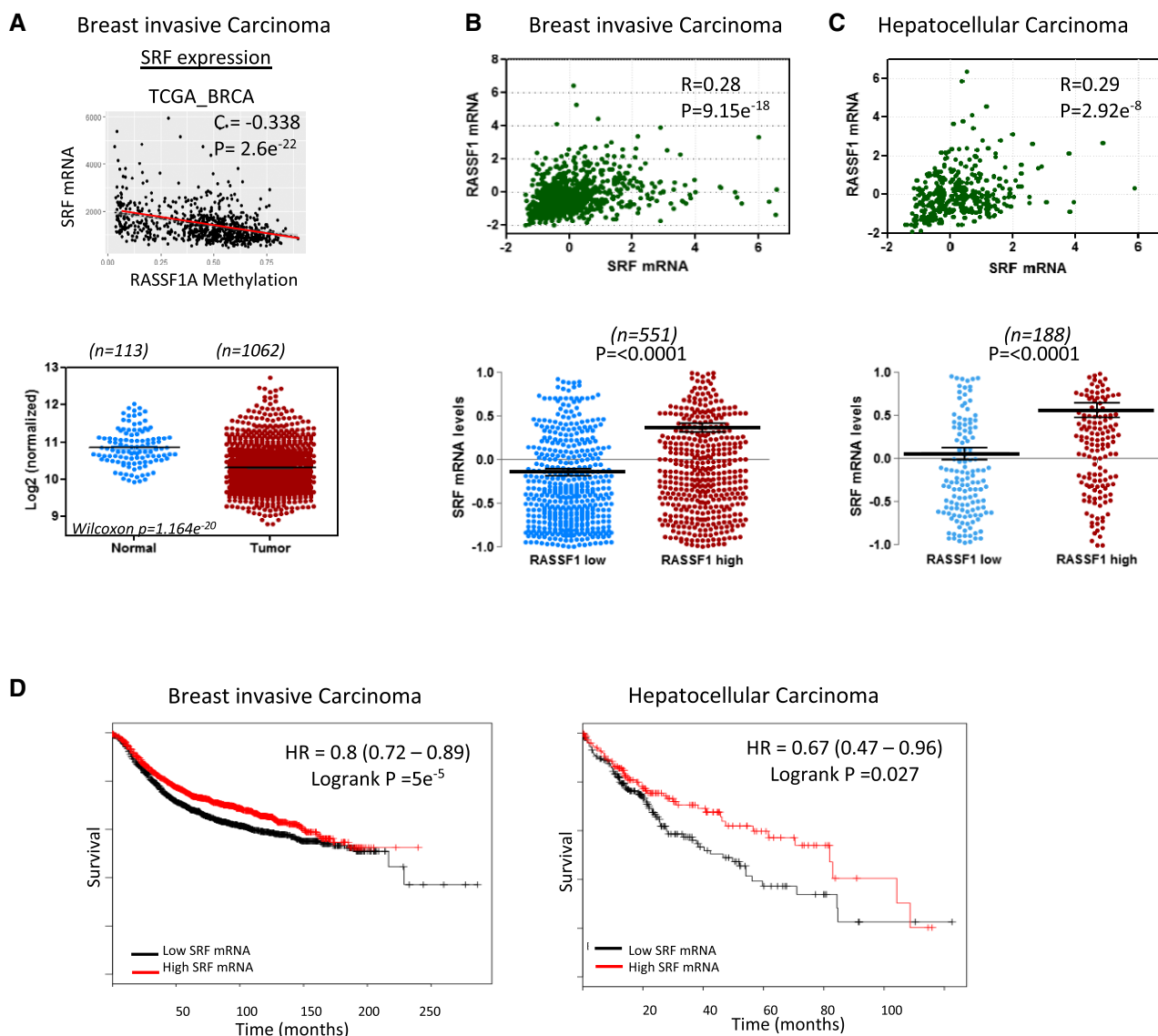


Figure 6. Correlation of RASSF1 and SRF expression in human tumours.

A Upper: scatter plot of RASSF1 methylation levels to SRF mRNA expression in breast invasive carcinoma (TCGA, Provisional, $n = 960$). Lower: SRF expression (TCGA, Illumina HiSeq RNA Seq) in normal and BRCA patients.

B Upper: scatter plot of RASSF1 mRNA to SRF mRNA levels in breast invasive carcinoma (TCGA, Provisional, $n = 960$). Values are given in (RNA Seq V2 RSEM). Lower: differences in SRF mRNA expression of samples that express low and high levels of RASSF1 mRNA.

C Upper: scatter plot of RASSF1 mRNA to SRF mRNA levels in hepatocellular carcinoma (TCGA, Provisional, $n = 360$ samples). Values are given in (RNA Seq V2 RSEM). Lower: differences in SRF mRNA expression of samples that express low and high levels of RASSF1 mRNA.

D Survival analysis of BRCA ($n = 3,951$) and HCC ($n = 364$) patient samples estimated by Kaplan–Meier survival curve with high (red) and low (black) expression of SRF.

mechanisms, but this remains unexplained. Intriguingly, nuclear actin levels have also been described to contribute to the regulation of Hippo pathway (e.g. SRF regulation of YAP; Sen *et al*, 2015; Foster *et al*, 2017), apoptosis (Sharili *et al*, 2016), differentiation (Xu *et al*, 2010; Sen *et al*, 2015, 2017) and DNA damage/repair (Yuan & Shen, 2001; Belin *et al*, 2015). Altogether, our findings indicate that loss of RASSF1A expression results in failure to export nuclear actin, suggesting that both regulatory processes are linked and that the clinical data associated with RASSF1 methylation involve deregulated MRTF-A/SRF.

Materials and Methods

Tissue culture and cell treatments

HeLa, MEFs, HEK293, RPE-1 and MDA-MB-231 cells were cultured in complete DMEM supplemented with 10% foetal bovine serum in 5% CO₂ and 20% O₂ at 37°C. HeLa cells were purchased from Cancer Research UK, London, or LGC Promochem (ATCC). Inhibitors for ATR kinase activity (VE-821) and ataxia-telangiectasia-mutated (ATM) kinase activity (KU-55933) were used at a

concentration of 10 μ M. 10 μ M 5-aza-2'-deoxycytidine (5'-aza-dC; Sigma) was added to the medium, and the cells were incubated for 72 h. Due to its chemical instability, 5'-aza-dC was added to the fresh medium every 24 h.

Real-time PCR primers

Target gene	Forward	Reverse
PAK1	ACCACCAGTGATTGCTCCAC	GCATCTGGTGGAGTGGTGT
ITGB1	TCCAACCTGATCTGTGTCC	CAATCCAGCAACCACACCA
MYL9	GTTTGGGAGAAGCTGAACG	CCGGTACATCTCGTCCACTT
GAPDH	AACGGGAAGCTTGTCATCA	CCCAGCCTTCTCCATGGTG
OCT4	GGTCCGAGTGTGTTCTGTA	CGAGGAGTACAGTGCAGTGA
SRF	GGAGACCAAGGACACACTGA	TGCCTGTACTCTTCAGCACA
IPO9	TGGGTGAGAGCAGAAGGTCT	CTTCTGCTGACACTGGACA

siRNA oligonucleotides

RNA interference was carried out with 100 nM siRNA for 48 h using Lipofectamine 2000 (Invitrogen) according to manufacturer's instructions. The oligos used were as follows: siMST2: siGENOME SMARTpool: M-004874-02 (Dharmacon), siRASSF1A: GACCUCU-GUGGCGACUU, siLaminA/C: sc35776 (Santa Cruz Biotechnology, Inc), siIPO9: EHU102331 (Sigma). siRNA against luciferase with the sequence GCCAUUCUAUCCUCUAGAGGAUG was used as control.

Plasmids

RASSF1A truncation mutants, MYC-RASSF1A 1–288, MYC-RASSF1A 120–340 and MYC-RASSF1A120–288, were created by PCR using MYC-tagged RASSF1A as template, as previously shown (Pefani *et al*, 2016). MDA-MB-231 cells were transiently transfected with 1 μ g of RASSF1A DNA or the empty pcDNA 3.0 plasmid using Lipofectamine 2000 (Invitrogen).

Antibodies

The following antibodies were used in this study: RASSF1A (Atlas, HPA040735), MST1 (Sigma, WH0006789M1), MST2 (Abcam, ab71960, ab52641), XPO6 (Bethyl, A301-205A), CRM1 (Cell Signaling, 46249), XPO4 (Novus Biologicals, NB100-56495), XPO5 (sc-166789), XPO7 (sc-390025), Lamin A/C (Cell Signaling, 4777), Lamin B (Abcam, ab16048), Profilin (Novus Biologicals, NBP2-02577), IPO9 (Abcam, ab52605), Myc-Tag (JBW301, Millipore, 05-724), GAPDH (Cell Signaling, 97166), Actin (sc-1616, Santa Cruz), RAN (Santa Cruz Biotechnology, sc58467), MRTF-A (Santa Cruz Biotechnology, sc-398675), α -tubulin (Abcam, ab7291) and pS131-RASSF1A custom-made (Hamilton *et al*, 2009).

Quantitative real-time PCR analysis

RNA extraction, reverse transcription and qPCR were performed using the Ambion Power SYBR Green Cells-to-CT kit following manufacturer's instructions in a 7500 FAST Real-Time PCR

thermocycler with v2.0.5 software (Applied Biosystems). The mRNA expression level of each gene relative to GAPDH was calculated using the $\Delta\Delta C_t$ method. All experiments were performed in triplicates.

Protein extraction and immunoblotting

Cytosolic and nuclear fractions were prepared using the NE-PER Nuclear and Cytosolic Extraction Reagents (Thermo Fisher Scientific) according to the manufacturer's instructions. Sample protein content was determined by the bicinchoninic acid assay protein assay (Thermo Fisher Scientific). Extracts were analysed by SDS-PAGE using a 10% Bis-Tris NuPAGE gels (Invitrogen) and transferred onto PVDF membranes (Millipore). Subsequent to being washed with PBS containing 1% Tween-20 (PBS-T), the membranes were blocked in 5% bovine serum albumin (BSA) in TBS-T for 1 h at RT and then incubated with the primary antibody overnight at 4°C. The membranes were incubated with HRP-conjugated secondary antibodies for 1 h at room temperature and exposed to X-ray film (Kodak) after incubation with Thermo Scientific Pierce ECL or Amersham ECL (GE Healthcare). ImageJ software (NIH) was used for the quantification of the bands. All bands were normalised against the loading controls.

Immunofluorescence

HeLa cells were grown on coverslips, washed with PBS and fixed with MeOH at 20°C for 20 min. Where indicated, cells were instead fixed in 4% paraformaldehyde and permeabilised either with 0.5% Triton X-100 at room temperature for 5 min or with 40 μ g/ml digitonin on ice for 2 min. Coverslips were then incubated with primary antibody for 2 h in PBS with 3% BSA at room temperature. Cells were washed with PBS and incubated with secondary anti-rabbit and/or anti-mouse or anti-rat IgG conjugated with Alexa Fluor 488 or Alexa Fluor 568 (Molecular Probes) for 1 h at room temperature. Samples were washed and mounted on coverslips with mounting medium containing DAPI (Invitrogen). For the visualisation of F- and G-actin, cells were fixed with 4% paraformaldehyde, permeabilised with 100% acetone at 20° for 5 min and stained with Alexa Fluor 568 Phalloidin or Alexa Fluor 488 DNase I, respectively. Cells were analysed using LSM780 (Carl Zeiss Microscopy) confocal microscope. Fluorescence intensity plots were generated using ImageJ software (NIH).

Immunoprecipitation

Cells were lysed in lysis buffer [50 mM Tris-HCl pH 7.5, 0.15 M NaCl, 1 mM EDTA, 1% NP-40, 1 mM Na_3VO_4 , complete proteinase inhibitor cocktail (Roche)] and incubated with 20 μ l protein G Dynabeads (Invitrogen) and 2 μ g of the indicated antibodies at for 2 h at 4°C. Pelleted beads were collected in sample buffer NuPAGE LDS (Thermo Fisher Scientific) with 200 mM DTT and subjected to SDS-PAGE and immunoblotting.

GST pull-down assay

HeLa cells transfected with siCTRL or siRASSF1A were lysed in lysis buffer (25 mM Tris-HCl, pH 7.2, 150 mM NaCl, 5 mM MgCl_2 , 1%

NP-40 and 5% glycerol). 20 µg of GST-RAN was mixed with 500 µg of lysates in spin cups (Thermo Fisher Scientific #69700) containing 40 µl of 50% glutathione-agarose beads (Thermo Fisher Scientific #16100). The samples were rotated for at least 1 h at 4°C. The beads were washed five times with the lysis buffer, mixed with 40 µl of 2× Laemmli buffer and boiled for 10 min at 95°C. The beads were pelleted and the supernatant used for analysis via SDS–PAGE and Western blot. GST-RAN recombinant protein was purchased from Novus Biologicals.

Mass spectrometry

HeLa cells were lysed in 1% NP-40 lysis buffer (150 mM NaCl, 20 mM HEPES, 0.5 mM EDTA) containing complete protease and phosphatase inhibitor cocktail (Roche). 10 mg of total protein lysate was incubated for 3 h with protein A Dynabeads (Invitrogen) and 10 µg of MST2 antibody (ab52641) or rIgG at 4°C. MST2 immunoprecipitates were eluted off the beads in a low pH glycine buffer. The eluted fractions were sequentially incubated with DTT (5 mM final concentration) and Iodoacetamide (20 mM final concentration) for 30 min at room temperature in the dark, before proteins were precipitated with methanol/chloroform. Protein precipitates were reconstituted and denatured with 8 M urea in 20 mM HEPES (pH 8). Samples were then further diluted to a final urea concentration of 2 M using 20 mM HEPES (pH 8.0) before adding immobilised trypsin for 16 h at 37°C (Pierce 20230; Montoya *et al* 2011). Trypsin digestion was stopped by adding 1% TFA (final concentration) and trypsin beads removed by centrifugation. Tryptic peptides solution was desalted by solid-phase extraction using C18 Spin Tips (Glygen LTD) and dried down.

Dried tryptic peptides were reconstituted in 15 µl of LC-MS grade water containing 2% acetonitrile and 0.1% TFA. Seven per cent of the sample was analysed by liquid chromatography–tandem mass spectrometry (LC-MS/MS) using a Dionex UltiMate 3000 UPLC coupled to a Q-Exactive mass spectrometer (Thermo Fisher Scientific). Peptides were loaded onto a trap column (PepMap C18; 300 µm × 5 mm, 5 µm particle size, Thermo Fisher) for 1 min at a flow rate of 20 µl/min before being chromatographic separated on a 50-cm-long Easy-Spray Column (ES803, PepMAP C18, 75 µm × 500 mm, 2 µm particle, Thermo Fisher) with a gradient of 2–35% acetonitrile in 0.1% formic acid and 5% DMSO with a 250 nl/min flow rate for 60 min (Chung *et al* 2016). The Q-Exactive was operated in a data-dependent acquisition (DDA) mode to automatically switch between full MS scan and MS/MS acquisition. Survey-full MS scans were acquired in the Orbitrap mass analyser over an *m/z* window of 380–1,800 and at a resolution of 70 k (AGC target at 3e6 ions). Prior to MSMS acquisition, the top 15 most intense precursor ions (charge state ≥ 2) were sequentially isolated in the Quad (*m/z* 1.6 window) and fragmented in the HCD collision cell (normalised collision energy of 28%). MS/MS data were obtained in the Orbitrap at a resolution of 17,500 with a maximum acquisition time of 128 ms, an AGC target of 1e5 and a dynamic exclusion of 27 s.

The raw data were searched against the Human UniProt–SwissProt database (November 2015; containing 20,268 human sequences) using Mascot data search engine (v2.3). The search was carried out by enabling the Decoy function, whilst selecting trypsin as enzyme (allowing 1 missed cleavage), peptide charge of +2, +3, +4 ions, peptide tolerance of 10 ppm and MS/MS of 0.05 Da; #13C at 1; carbamidomethyl (C) as fixed modification; and oxidation (M) and deamidation (NQ) as a variable modification. MASCOT outputs

were filtered using an ion score cut-off of 20 and a false discovery rate (FDR) of 1%.

Cell adhesion assay

HeLa cells were transfected with siRNA against RASSF1A or RASSF1A and IPO9 or control and were collected after 48 h. 1×10^5 cells were re-plated on fibronectin-coated 24-well plate in triplicate. After attachment for the predetermined time (30, 60 and 90 min), the plate was washed to remove the non-adherent cells. The number of adherent cells from four random fields of the well was counted microscopically.

SRF reporter assay

Cells were transfected with the SRF luciferase reporter (pGL4.34) using Lipofectamine 2000. pRL Renilla luciferase vector was used as an internal control. Following DNA transfection, cells were rinsed and cultured for 24 h before treating with FBS. Luciferase assays were carried out in 24-well plates ($n = 3$ wells); cells were treated for 7 h with FBS, then harvested and analysed using the dual luciferase assay (Promega).

Correlation analysis

The TCGA data were downloaded from the cBioPortal for Cancer Genomics (<http://www.cbioportal.org>). The association of RNA expression of RASSF1 and SRF was studied in breast invasive carcinoma (TCGA, Provisional), hepatocellular carcinoma (TCGA, Provisional), bladder cancer (Robertson *et al* 2017) and colorectal adenocarcinoma (Cancer Genome Atlas Network 2012). Methylation 450K data and gene expression data were downloaded from TCGA (BRCA). RASSF1A methylation levels for each patient were determined as the average beta value across all probes within the RASSF1A CpG island (chr3:50377804–50378540). Pearson correlation and scatter plots were drawn using R (Ver 3.4). Survival analyses from 3951 BRCA samples and 364 liver HCC patient samples were performed using the Kaplan–Meier Plotter tool with the patients being split by median (Nagy *et al*, 2018).

Statistics

Statistical analysis was performed with the GraphPad Prism 7 software. For all experiments, statistical analysis was carried out using Student's *t*-test. All data are expressed as mean ± SEM.

Data availability

The mass spectrometry raw data included from this publication have been deposited to the ProteomeXchange Consortium via the PRIDE partner repository and assigned the identifier PRIDE: PXD11517 (<https://www.ebi.ac.uk/pride/archive/projects/PXD11517>).

Expanded View for this article is available online.

Acknowledgements

This work was funded by Cancer Research UK A19277. Dafni Eleftheria Pefani is funded by the Hellenic Foundation for Research and Innovation (HFRI) and

the General Secretariat for Research and Technology (GSRT), under grant agreement No [775]. Mass spectrometry analysis was performed at the Discovery Proteomics Facility (headed by Roman Fischer) which is part of the TDI MS Laboratory (led by Benedikt Kessler).

Author contributions

MC conceived the project and designed the research, performed experiments and analysed data. D-EP, DP and ME assisted with experiments. IV and RF performed the mass spectrometry analysis. EON and MC wrote the manuscript.

Conflict of interest

The authors declare that they have no conflict of interest.

References

- Avruch J, Praskova M, Ortiz-Vega S, Liu M, Zhang X (2006) Nore1 and RASSF1 regulation of cell proliferation and of the MST1/2 kinases. *Methods enzymol* 407: 290–310
- Baarlink C, Wang H, Grosse R (2013) Nuclear actin network assembly by formins regulates the SRF coactivator MAL. *Science* 340: 864–867
- Baksh S, Tommasi S, Fenton S, Yu VC, Martins LM, Pfeifer GP, Latif F, Downward J, Neel BG (2005) The tumor suppressor RASSF1A and MAP-1 link death receptor signaling to bax conformational change and cell death. *Mol Cell* 18: 637–650
- Belin BJ, Lee T, Mullins RD (2015) DNA damage induces nuclear actin filament assembly by formin-2 and spire-1/2 that promotes efficient DNA repair. *eLife* 4: e07735
- Bompard G, Rabeharivelo G, Frank M, Cau J, Delsert C, Morin N (2010) Subgroup II PAK-mediated phosphorylation regulates Ran activity during mitosis. *J Cell Biol* 190: 807–822
- de Boor S, Knyphausen P, Kuhlmann N, Wroblewski S, Brenig J, Scislawski L, Baldus L, Nolte H, Krüger M, Lammers M (2015) Small GTP-binding protein Ran is regulated by posttranslational lysine acetylation. *Proc Natl Acad Sci USA* 112: E3679–E3688
- Cancer Genome Atlas Network (2012) Comprehensive molecular characterization of human colon and rectal cancer. *Nature* 487: 330
- Chung VY, Konietzny R, Charles P, Kessler B, Fischer R, Turney BW (2016) Proteomic changes in response to crystal formation in *Drosophila* Malpighian tubules. *Fly* 10: 91–100
- Ciasca G, Papi M, Minelli E, Palmieri V, De Spirito M (2016) Changes in cellular mechanical properties during onset or progression of colorectal cancer. *World J Gastroenterol* 22: 7203
- Cui Y, Hameed FM, Yang B, Lee K, Pan CQ, Park S, Sheetz M (2015) Cyclic stretching of soft substrates induces spreading and growth. *Nat Commun* 6: 6333
- Dallol A, Agathangelou A, Fenton SL, Ahmed-Choudhury J, Hesson L, Vos MD, Clark GJ, Downward J, Maher ER, Latif F (2004) RASSF1A interacts with microtubule-associated proteins and modulates microtubule dynamics. *Cancer Res* 64: 4112–4116
- Dallol A, Hesson LB, Matallanas D, Cooper WN, O'Neill E, Maher ER, Kolch W, Latif F (2009) RAN GTPase is a RASSF1A effector involved in controlling microtubule organization. *Curr Biol* 19: 1227–1232
- Dittfeld C, Richter AM, Steinmann K, Klagge-Ulonska A, Dammann RH (2012) The SARAH domain of RASSF1A and its tumor suppressor function. *Mol Biol Int* 2012: 196715
- Donninger H, Clark J, Rinaldo F, Nelson N, Barnoud T, Schmidt ML, Hobbing KR, Vos MD, Sils B, Clark GJ (2015) The RASSF1A tumor suppressor regulates XPA-mediated DNA repair. *Mol Cell Biol* 35: 277–287
- Dopie J, Skarp K-P, Rajakylä EK, Tanhuanpää K, Vartiainen MK (2012) Active maintenance of nuclear actin by importin 9 supports transcription. *Proc Natl Acad Sci USA* 109: E544–E552
- Egley JM, Miyamoto NG, Moncollin V, Chambon P (1984) Is actin a transcription initiation factor for RNA polymerase B? *EMBO J* 3: 2363–2371
- El-Kalla M, Onyskiw C, Baksh S (2010) Functional importance of RASSF1A microtubule localization and polymorphisms. *Oncogene* 29: 5729–5740
- Fiore APZP, Spencer VA, Mori H, Carvalho HF, Bissell MJ, Bruni-Cardoso A (2017) Laminin-111 and the level of nuclear actin regulate epithelial quiescence via exportin-6. *Cell Rep* 19: 2102–2115
- Fornerod M, Ohno M, Yoshida M, Mattaj JW (1997) CRM1 is an export receptor for leucine-rich nuclear export signals. *Cell* 90: 1051–1060
- Foster CT, Gualdrini F, Treisman R (2017) Mutual dependence of the MRTF-SRF and YAP-TEAD pathways in cancer-associated fibroblasts is indirect and mediated by cytoskeletal dynamics. *Genes Dev* 31: 2361–2375
- Ghosh K, Thodeti CK, Dudley AC, Mammoto A, Klagsbrun M, Ingber DE (2008) Tumor-derived endothelial cells exhibit aberrant Rho-mediated mechanosensing and abnormal angiogenesis *in vitro*. *Proc Natl Acad Sci USA* 105: 11305–11310
- Grawenda AM, O'Neill E (2015) Clinical utility of RASSF1A methylation in human malignancies. *Br J Cancer* 113: 372–381
- Grosse R, Vartiainen MK (2013) To be or not to be assembled: progressing into nuclear actin filaments. *Nat Rev Mol Cell Biol* 14: 693–697
- Guilluy C, Osborne LD, Van Landeghem L, Sharek L, Superfine R, Garcia-Mata R, Burridge K (2014) Isolated nuclei adapt to force and reveal a mechanotransduction pathway in the nucleus. *Nat Cell Biol* 16: 376–381
- Guo C, Tommasi S, Liu L, Yee JK, Dammann R, Pfeifer GP (2007) RASSF1A is part of a complex similar to the *Drosophila* Hippo/Salvador/Lats Tumor-Suppressor Network. *Curr Biol* 17: 700–705
- Güttler T, Görlich D (2011) Ran-dependent nuclear export mediators: a structural perspective. *EMBO J* 30: 3457–3474
- Hamilton G, Yee KS, Scrase S, O'Neill E (2009) ATM regulates a RASSF1A-dependent DNA damage response. *Curr Biol* 19: 2020–2025
- Ho CY, Jaalouk DE, Vartiainen MK, Lammerding J (2013) Lamin A/C and emerin regulate MKL1-SRF activity by modulating actin dynamics. *Nature* 497: 507–511
- Hofmann WA, Stojiljkovic L, Fuchsova B, Vargas GM, Mavrommatis E, Philimonenko V, Kysela K, Goodrich JA, Lessard JL, Hope TJ et al (2004) Actin is part of pre-initiation complexes and is necessary for transcription by RNA polymerase II. *Nat Cell Biol* 6: 1094–1101
- Honda K (2015) The biological role of actinin-4 (ACTN4) in malignant phenotypes of cancer. *Cell Biosci* 5: 41
- Kapoor P, Shen X (2014) Mechanisms of nuclear actin in chromatin-remodeling complexes. *Trends Cell Biol* 24: 238–246
- Khurana S, Chakraborty S, Cheng X, Su Y-T, Kao H-Y (2011) The actin-binding protein, actinin alpha 4 (ACTN4), is a nuclear receptor coactivator that promotes proliferation of MCF-7 breast cancer cells. *J Biol Chem* 286: 1850–1859
- Liu L, Tommasi S, Lee DH, Dammann R, Pfeifer GP (2003) Control of microtubule stability by the RASSF1A tumor suppressor. *Oncogene* 22: 8125–8136
- Loy CJ, Sim KS, Yong EL (2003) Filamin-A fragment localizes to the nucleus to regulate androgen receptor and coactivator functions. *Proc Natl Acad Sci USA* 100: 4562–4567

- Matallanas D, Romano D, Yee K, Meissl K, Kucerova L, Piazzolla D, Baccarini M, Vass JK, Kolch W, O'Neill E (2007) RASSF1A elicits apoptosis through an MST2 pathway directing proapoptotic transcription by the p73 tumor suppressor protein. *Mol Cell* 27: 962–975
- Miralles F, Posern G, Zaromytidou AI, Treisman R (2003) Actin dynamics control SRF activity by regulation of its coactivator MAL. *Cell* 113: 329–342
- Montenegro MF, Sáez-Ayala M, Piñero-Madrona A, Cabezas-Herrera J, Rodríguez-López JN (2012) Reactivation of the tumour suppressor RASSF1A in breast cancer by simultaneous targeting of DNA and E2F1 methylation. *PLoS One* 7: e52231
- Montoya A, Beltran L, Casado P, Rodríguez-Prados JC (2011) Characterization of a TiO₂ enrichment method for label-free quantitative phosphoproteomics. *Methods* 54: 370–378
- Nagy Á, Lánckzy A, Menyhárt O, Györfy B (2018) Validation of miRNA prognostic power in hepatocellular carcinoma using expression data of independent datasets. *Sci Rep* 8: 9227
- Papaspapropoulos A, Bradley L, Thapa A, Leung CY, Toskas K, Koennig D, Pefani D-E, Raso C, Grou C, Hamilton G et al (2018) RASSF1A uncouples Wnt from Hippo signalling and promotes YAP mediated differentiation via p73. *Nat Commun* 9: 424
- Patnaik S, George SP, Pham E, Roy S, Singh K, Mariadason JM, Khurana S (2016) By moonlighting in the nucleus, villin regulates epithelial plasticity. *Mol Biol Cell* 27: 535–548
- Pefani DE, Latusek R, Pires I, Grawenda AM, Yee KS, Hamilton G, Van Der Weyden L, Esashi F, Hammond EM, O'Neill E (2014) RASSF1A-LATS1 signalling stabilizes replication forks by restricting CDK2-mediated phosphorylation of BRCA2. *Nat Cell Biol* 16: 962–971
- Pefani DE, Pankova D, Abraham AG, Grawenda AM, Vlahov N, Scrase S, O'Neill E (2016) TGF- β targets the Hippo pathway Scaffold RASSF1A to facilitate YAP/SMAD2 nuclear translocation. *Mol Cell* 63: 156–166
- Pefani DE, Tognoli ML, Pirincci Ercan D, Gorgoulis V, O'Neill E (2018) MST2 kinase suppresses rDNA transcription in response to DNA damage by phosphorylating nucleolar histone H2B. *EMBO J* 37: e98760
- Philimonenko VV, Zhao J, Iben S, Dingová H, Kyselá K, Kahle M, Zentgraf H, Hofmann WA, de Lanerolle P, Hozák P et al (2004) Nuclear actin and myosin I are required for RNA polymerase I transcription. *Nat Cell Biol* 6: 1165–1172
- Posern G, Sotiropoulos A, Treisman R (2002) Mutant actins demonstrate a role for unpolymerized actin in control of transcription by serum response factor. *Mol Biol Cell* 13: 4167–4178
- Qi T, Tang W, Wang L, Zhai L, Guo L, Zeng X (2011) G-actin participates in RNA polymerase II-dependent transcription elongation by recruiting positive transcription elongation factor b (P-TEFb). *J Biol Chem* 286: 15171–15181
- Robertson AG, Kim J, Al-Ahmadie H, Bellmunt J, Guo G, Cherniack AD, Hinoue T, Laird PW, Hoadley KA, Akbani R, et al. (2017) Comprehensive molecular characterization of muscle-invasive bladder cancer. *Cell* 171: 540–556
- Sánchez-Sanz G, Matallanas D, Nguyen LK, Kholodenko BN, Rosta E, Kolch W, Buchete N-V (2016) MST2-RASSF protein–protein interactions through SARAH domains. *Brief Bioinform* 17: 593–602
- Savoy RM, Ghosh PM (2013) The dual role of filamin A in cancer: can't live with (too much of) it, can't live without it. *Endocr Relat Cancer* 20: R341–R356
- Sen B, Xie Z, Uzer G, Thompson WR, Styner M, Wu X, Rubin J (2015) Intracellular actin regulates osteogenesis. *Stem Cells* 33: 3065–3076
- Sen B, Uzer G, Samsonraj RM, Xie Z, McGrath C, Styner M, Dudakovic A, van Wijnen AJ, Rubin J (2017) Intracellular actin structure modulates mesenchymal stem cell differentiation. *Stem Cells* 35: 1624–1635
- Sharili AS, Kenny FN, Vartiainen MK, Connelly JT (2016) Nuclear actin modulates cell motility via transcriptional regulation of adhesive and cytoskeletal genes. *Sci Rep* 6: 33893
- Sherwood V, Recino A, Jeffries A, Ward A, Chalmers AD (2010) The N-terminal RASSF family: a new group of Ras-association-domain-containing proteins, with emerging links to cancer formation. *Biochem J* 425: 303–311
- Sotiropoulos A, Gineitis D, Copeland J, Treisman R (1999) Signal-regulated activation of serum response factor is mediated by changes in actin dynamics. *Cell* 98: 159–169
- Stuven T, Hartmann E, Görlisch D (2003) Exportin 6: a novel nuclear export receptor that is specific for profilin{middle dot}actin complexes. *EMBO J* 22: 5928–5940
- Tang X, Wen Q, Kuhlenschmidt TB, Kuhlenschmidt MS, Janmey PA, Saif TA (2012) Attenuation of cell mechanosensitivity in colon cancer cells during *in vitro* metastasis. *PLoS One* 7: e50443
- Vartiainen MK, Guettler S, Larijani B, Treisman R (2007) Nuclear actin regulates dynamic subcellular localization and activity of the SRF cofactor MAL. *Science* 316: 1749–1752
- Velkova A, Carvalho MA, Johnson JO, Tavtigian SV, Monteiro ANA (2010) Identification of Filamin A as a BRCA1-interacting protein required for efficient DNA repair. *Cell Cycle* 9: 1421–1433
- Visa N, Percipalle P (2010) Nuclear functions of actin. *Cold Spring Harb Perspect Biol* 2: 1–14
- Vlahov N, Scrase S, Soto MS, Grawenda AM, Bradley L, Pankova D, Papaspapropoulos A, Yee KS, Buffa F, Goding CR et al (2015) Alternate RASSF1 transcripts control SRC activity, E-Cadherin contacts, and YAP-mediated invasion. *Curr Biol* 25: 3019–3034
- Vos MD, Ellis CA, Bell A, Birrer MJ, Clark GJ (2000) Ras uses the novel tumor suppressor RASSF1 as an effector to mediate apoptosis. *J Biol Chem* 275: 35669–35672
- Vos MD, Martinez A, Elam C, Dallol A, Taylor BJ, Latif F, Clark GJ (2004) A role for the RASSF1A tumor suppressor in the regulation of tubulin polymerization and genomic stability. *Cancer Res* 64: 4244–4250
- Xu YZ, Thuraingam T, de Lima Moraes DA, Rola-Pleszczynski M, Radzioch D (2010) Nuclear translocation of β -actin is involved in transcriptional regulation during macrophage differentiation of HL-60 cells. *Mol Biol Cell* 21: 811–820
- Yamazaki S, Yamamoto K, Tokunaga M, Sakata-Sogawa K, Harata M (2015) Nuclear actin activates human transcription factor genes including the OCT4 gene. *Biosci Biotechnol Biochem* 79: 242–246
- Yuan Y, Shen Z (2001) Interaction with BRCA2 suggests a role for filamin-1 (hsFLN1) in DNA damage response. *J Biol Chem* 276: 48318–48324



License: This is an open access article under the terms of the Creative Commons Attribution 4.0 License, which permits use, distribution and reproduction in any medium, provided the original work is properly cited.